文章编号：1001-9014(2022)05-0844-06

DOI:10.11972/j.issn.1001-9014.2022.05.007

Distortions of terahertz pulses induced by the air coherent detection technique

DU Hai-Wei[1,2,3*], LONG Jiang[3]

(1. Key Laboratory of Nondestructive Testing Technology (Ministry of Education), Nanchang Hangkong University, Nanchang 330063, China;
2. Key Laboratory of Opto-Electronic Information Science and Technology of Jiangxi Province, Nanchang Hangkong University, Nanchang 330063, China;
3. School of Measuring and Optical Engineering, Nanchang Hangkong University, Nanchang 330063, China)

Abstract: Terahertz air coherent detection technique is a broadband detection method, which has been widely used in the broadband terahertz technology after its demonstration in the experiment. The frequency response of this method is determined by the duration of the probe laser pulse. Thus, the different probe lasers might induce distortions of terahertz pulses during the detection process. In this paper, the distortions and the energy loss of the terahertz pulses induced by the air coherent detection technique are quantitatively investigated based on the simulations. The results show that the pulse distortions and the energy loss depend on the duration of the probe laser pulse and the central frequency of terahertz pulse to be detected. This work will help to estimate the influence of the air coherent detection technique in the broadband terahertz technology.

Key words: terahertz, broadband, air coherent detection, distortion

太赫兹空气相干探测技术引起的太赫兹脉冲畸变

杜海伟[1,2,3*], 龙 江[3]

(1. 南昌航空大学 无损检测技术教育部重点实验室,江西 南昌 330063;
2. 江西省光电信息科学与技术重点实验,江西 南昌 330063;
3. 南昌航空大学 测试与光电工程学院,江西 南昌 330063)

摘要:太赫兹空气相干探测技术是一种宽带探测技术,目前已被广泛应用于宽带太赫兹技术中。该技术的频率响应由探测激光脉冲宽度决定。因此,不同的探测激光脉冲在探测过程可能引起太赫兹脉冲的畸变。本文基于数值计算研究了空气相干探测技术引起的太赫兹脉冲的脉冲畸变和能量损失。结果显示,这种脉冲畸变和能量损失主要依赖探测激光脉冲宽度和待探测的太赫兹脉冲的中心频率。本项工作对于估测在宽带太赫兹技术中使用空气相干探测技术的性能和表现有很好的帮助。

关 键 词:太赫兹;宽带;空气相干探测技术;畸变

中图分类号:O434.3　　**文献标识码**:A

Introduction

Terahertz (THz) wave, as a special electromagnetic wave between the microwave and the far infrared, whose frequency covers the bandwidth from 0.1~10 THz (1 THz $=10^{12}$ Hz), has shown its huge applications in the industry and the basic research areas[1-2]. Its generation and detection are its applications' basic. Especially, the coherent detection techniques of THz wave can obtain its time waveform, the amplitude, and the phase simultaneously. Thus, the coherent detection techniques can make full use of the potential of THz wave and are significant for the THz spectroscopy[3]. There are three widely used THz coherent detection techniques, including pho-

Received date: 2021-09-02, **revised date**: 2022-03-05　　**收稿日期**:2021-09-02,**修回日期**:2022-03-05

Foundation items: Supported by the National Natural Science Foundation of China (12064028); Open Foundation of Key Laboratory of Nondestructive Testing Technology (Ministry of Education) (EW202108218).

Biography: DU Hai-Wei (1980-), male, Anyang Henan, associate professor, doctor. Research area involves terahertz science and technology, ultrafast optics, and laser plasma interaction. E-mail: haiweidu@nchu.edu.cn

* **Corresponding author**: E-mail: haiweidu@nchu.edu.cn

toconductor antenna (PCA)[4-5], electro-optic sampling (EOS)[6-7], and air coherent detection (air-biased-coherent-detection, ABCD)[8]. The detection limitations of the PCA and the EO are affected by their sensor materials, semiconductor and electro-optic crystal, respectively. Therefore, these two methods are hard to detect high frequency range of THz wave. While the last one employs the air/gas molecules as sensor, whose absorption and dispersion of the THz wave are small enough to be omitted. The frequency limitation of the air coherent detection technique is mainly affected by the duration of the probe laser pulse. Thus, it has huge advantage in the detection of broadband (especially super-broadband) THz radiation.

THz air coherent detection technique employs the THz field-induced laser second harmonic generation in the media[9], although the interaction between the laser plasma also generates the laser second harmonic during this process[10]. In the actual complementation of this technique, the probe laser pulse and the THz pulse are collinearly focused and overlap at the same point in the free space, where the air molecules work as sensor, then the probe laser pulse and the THz pulse jointly generate the laser second harmonic based on the four-wave-mixing effect. An external modulated biased field is set along the air sensor, offering a reference frequency to the lock-in amplifier, which makes this technique a coherent detection method[8]. Thus, this method is also named air-biased-coherent-detection (ABCD)[11].

Although the air coherent detection technique has been used to detect the broadband THz pulses, its frequency response is actually not smooth in the whole THz band. It is found that its response function has high sensitivity in the low frequency range and low sensitivity in the high frequency range, depending on the duration of the probe laser pulse[12]. Thus, this detection method might distort the THz pulses during the detection process, as that done by the electro-optic sampling method[13]. In this paper, the distortions and the energy loss of the broadband THz pulses induced by the air coherent detection technique are investigated based on the calculations. Several different THz pulses with different bandwidths and central frequencies are given to show these distortions and the energy loss. It is found that there is an obvious redshift for the broadband THz pulses depending on the duration of the probe laser pulses.

1 Response function of the THz air coherent detection technology

The response function of the air coherent detection technique is derived from the basic of the nonlinear optics, including the three-order polarization induced by the electric field and the response of the media[12]. The three-order polarization in the frequency domain is given as below

$$P^{(3)}(\omega,\Delta\tau)=\frac{1}{2\pi}\varepsilon_0\chi^{(3)}(\omega)E_{THz}(\Delta\tau)\,[A_0A^2(\omega)*E_0^2(\omega)], \quad (1)$$

where $\Delta\tau$ is the time delay between the THz pulse and the probe laser pulse, ε_0 is the permittivity of the vacuum, $\chi^{(3)}$ is the three-order susceptibility of the media in the frequency domain, E_{THz} is the field of the THz pulse, A_0 is the amplitude of the probe laser, $A(\omega)$ is the envelope of the probe laser, * denotes the convolution calculation, and E_0 is the field of the probe laser in the frequency domain. The oscillation of the THz pulses usually is long enough to be treated as a DC field comparing with the laser period, thus it is reasonable to control the THz field in the time domain by the time delay $\Delta\tau$. Usually, a probe laser pulse has its duration, the envelope, and the central frequency. Its ultrashort duration in the time domain determines that the Fourier transform of the envelope is also a pulse in the frequency domain, according to the uncertainty relationship. (The uncertainty relationship of quantum mechanisms in the time domain and the frequency domain has the expression: $\Delta t\cdot\Delta f\approx\hbar$, where Δt is the time duration of a pulse, Δf is its frequency bandwidth, and $\hbar$ is the Planck constant.). The property of the media is expressed via the susceptibility $\chi^{(3)}$:

$$\chi^{(3)}(\omega)=\int_0^\infty R^{(3)}(\tau)e^{-2i\omega\tau}d\tau \quad , \quad (2)$$

$R^{(3)}$ is the response of the media molecules/atoms in the pump field.

Eq. (1) shows that the three-order polarization $P^{(3)}$ in the frequency domain can be obtained by a convolution calculation when the envelope of the laser pulse and the property of the media (via $\chi^{(3)}$) are known. Then, the laser second harmonic produced by the four-wave mixing effect can be known its frequency response, whose central frequency is determined by the central frequency of the laser. The frequency bandwidth of the second harmonic is related to the square of the envelope.

The polarization of the media induced by the electric field usually includes two components: one is from the valence electrons and the other from the nuclei[14]. The response time of the former is on the order of subfemtosecond[15], and the latter is on the order of picosecond[16]. As a limitation of the ultrafast response of the media, a step function can be used to represent it:

$$\begin{cases} R^{(3)}(\tau)=C, \tau>0 \\ R^{(3)}(\tau)=0, \tau\leqslant 0 \end{cases} . \quad (3)$$

One femtosecond is short enough for a common femtosecond laser pulses (such as 50 fs), thus this approximation is reasonable.

Because there is a convolution calculation in the response function as above, it cannot give a response curve directly for the different probe lasers as the electro-optic sampling[17-18]. Thus, there is a fitted formula to calculate the full width at half maximum of the response function ($0.5R_{\max}$), $y=628/x$ with x in fs and y in THz. This helps to compare the theoretical results with the experimental ones[12]. Figure 1 shows this fitted curve and the convolution calculated results with different durations of the probe laser pulses. One can clearly see the relationship between the bandwidth of this response function and the duration of the probe laser pulse. For example, the

detection response bandwidth of a probe laser with 100 fs duration is close to 7 THz. Thus, the influence of the air coherent detection technique on the broadband THz pulses varies with the duration of the probe laser pulses. As a result, the distortions of THz pulses induced by this detection method varies with the probe laser pulses.

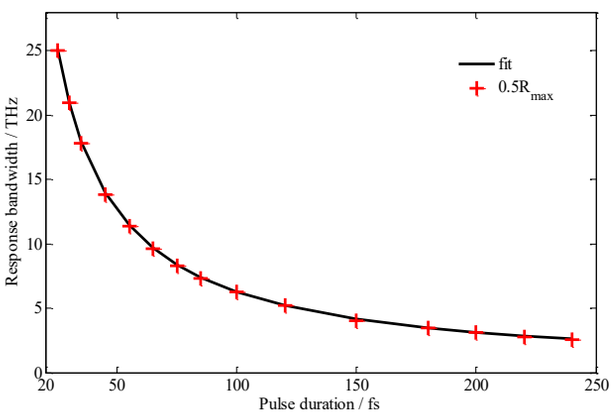

Fig. 1 The fitted curve of the response bandwidth of the air coherent detection technique with different pulse durations of the probe laser

图1 空气相干探测技术的响应带宽与探测激光脉冲宽度的拟合曲线

2 Distortion of THz pulses induced by the air coherent detection technology

As shown in Fig. 1 of Ref. [12], the response of the air coherent detection technique in the frequency range is not a smooth curve, but with a square of the Gaussian profile. Its sensitivity on all the frequency components of THz band is different. As a result, the detected broadband THz pulses by this technique produce some pulse distortions. We can calculate these distortions with given THz pulses as input signals. The detection technique with given probe laser reacts on the input signal as a special frequency function with its intrinsic response bandwidth.

Here, a THz pulse as an input signal is given by

$$E_{\mathrm{THz\_input}}(t) = \mathrm{e}^{-t^2/T_0^2}\cos(2\pi f_0 t + \varphi_0) \quad , \quad (4)$$

with a duration parameter T_0, a central frequency f_0 and an initial phase φ_0, in which T_0 and f_0 directly determine the duration and the bandwidth of the THz pulse. With this THz pulse as an input THz pulse to be detected, its frequency distribution $E_{\mathrm{THz}}(f)$ can be directly obtained by the Fourier transform:

$$E_{\mathrm{THz\_input}}(f) = \mathcal{F}\{E_{\mathrm{THz}}(t)\} \quad . \quad (5)$$

And then, the resultant output of the THz signal in the frequency range by the detection system is given by the product of the input signal and the response function of the detection system:

$$E_{\mathrm{THz\_output}}(f) = E_{\mathrm{THz\_input}}(f)R_{\mathrm{ABCD}}(f) \quad . \quad (6)$$

Here, $R_{\mathrm{ABCD}}(f)$ denotes the response function of the air coherent detection technique in the frequency domain, which is determined by the response of the polarization of the air/gas molecules, $R_{ABCD}(f) \propto P^{(3)}(2\pi f)$. $P^{(3)}$ is determined by Eq. (1) and the probe laser pulse. Finally, the time waveform of the THz pulse from the detection system is obtained by the inverse Fourier transform:

$$E_{\mathrm{THz\_output}}(t) = \mathcal{F}^{-1}\{E_{\mathrm{THz\_output}}(f)\} \quad . \quad (7)$$

Thus, the whole detection system as a frequency filter reacts on the THz pulses to be detected. It is easy to obtain such distortions induced by this detection method. This method also has been used to estimate the information of the electron bunches by monitoring its THz radiation through the electro-optic sampling[19-21]. The electro-optic sampling has its detection bandwidth limitation depending on the electro-optic crystal, although it has been used to coherent detection of the broadband THz radiation. If the THz signal to be detected produces some distortions by the detection method, its experimental results might lose some information and/or energy of the radiation. Therefore, it is significant to know these pulse distortions. One can estimate the waveform and the energy of true THz pulse from these distortions as well.

3 Calculations and discussions

In this section, the details of the distortions of THz pulses are given based on the calculations with the formulas above. Three kinds of broadband THz pulses are given with different bandwidths and central frequencies. Figure 2 shows these distortions with a THz pulse central frequency at 2 THz as input signal, (a) shows the time waveforms, (b) frequency spectra, and (c) their pulse energy loss. Four kinds of probe laser pulses with 50 fs, 100 fs, 150 fs, and 200 fs are used in the detection system. The input THz signal is in black as a comparison. As shown in Fig. 2(a), the waveforms of the THz pulses do not change obviously, but their frequencies have a redshift as shown in Fig. 2(b). In addition, the detection process makes some energy loss for this input signal. The energy of THz pulses after the detection is normalized with its initial pulse energy, as shown by Fig. 2(c). The results show that the energy loss is about 10% for the 50-fs probe laser, and gradually increase to 50% for the 200-fs probe laser.

When the input THz pulse increases its central frequency to 5 THz, the calculated results are given in Fig. 3, with the same kinds of the probe laser pulses as Fig. 2. Here, the redshift of the frequency becomes huge as shown in Fig. 3(b), its central frequency moving from 5 THz to 2.5 THz. And the energy loss increases from about 20% to 90% in Fig. 3(c). The pulse energy loss in the actual experiment is huge, and this indicates that a shorter probe laser pulse should be chosen for such broadband THz pulse.

Next, a super-broadband THz pulse with a central frequency of 8 THz is given as an input signal as well. Super-broadband THz pulse has its potential applications in the spectroscopy and analytical chemistry[22], and until now only the air coherent detection technique and the Michelson interference can work for such high frequency

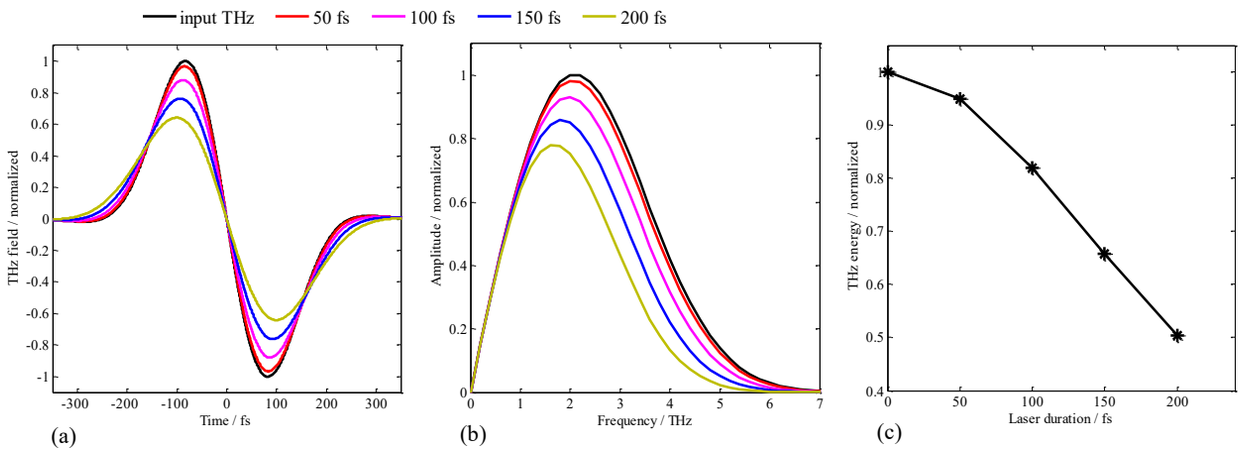

Fig. 2　The THz pulse distortions induced by air coherent detection technique with different probe laser pulses (50 fs, 100 fs, 150 fs, and 200 fs), the input THz pulse has a central frequency of 2 THz (black line), (a) shows their time waveforms, (b) shows their frequency spectra, and (c) shows their pulse energy loss, 0 fs duration in (c) means the initial normalized THz pulse energy

图2　在空气相干探测技术中使用不同脉宽(50 fs,100 fs,150 fs,200 fs)的探测激光引起的太赫兹脉冲畸变,待探测的太赫兹脉冲中心频率为2 THz,(a)为太赫兹脉冲波形,(b)为频谱分布,(c)为脉冲能量损失,(c)中0 fs代表归一化后的输入的太赫兹脉冲能量(下同)

THz range. Thus, it is necessary and useful to analyze the performance of them. Fig. 4 shows the THz waveforms, the frequency spectra, and the pulse energy loss after detection by the air coherent detection technique in (a), (b), and (c). As shown in Fig. 4(b), the frequency spectra have huge redshift, its central frequency moving from 8 THz to 2 THz when the probe laser pulses increase the duration from 50 fs to 200 fs. And its pulse energy loss even increases from 60% to 95%, which means that most of the THz pulse energy loses in the air coherent detection process with a 200-fs probe laser pulse.

In order to see the evolutions of the redshift and the energy loss of the THz pulses induced by different probe laser pulses, we employ the THz signals with the central frequencies from 1 THz to 10 THz, and the probe laser pulses with the duration from 30 fs to 220 fs. The frequency shift is defined as the difference between the central frequency of the input THz pulse and the output THz pulse, and its unit is THz. The results are plotted in two-dimensional colorful figures, as shown by Fig. 5(a) the frequency shift, and Fig. 5(b) the pulse energy loss. It is easy to see that: (1) the redshift of the normal broadband THz pulses (1~2 THz) is small with the probe laser from 30 fs to 220 fs; (2) when the THz pulse increase its central frequency from about 3 THz, this redshift cannot be ignored; (3) the energy loss can be ignored for the 1 THz pulse with 30~50 fs probe laser pulses, but should be considered for longer probe laser pulses; (4) the energy loss of the high frequency THz pulses is huge. Thus, Fig. 5 can offer useful clues to estimate the true property of a new broadband THz radiation source with the air coherent detection technique.

Since the air coherent detection technique has its de-

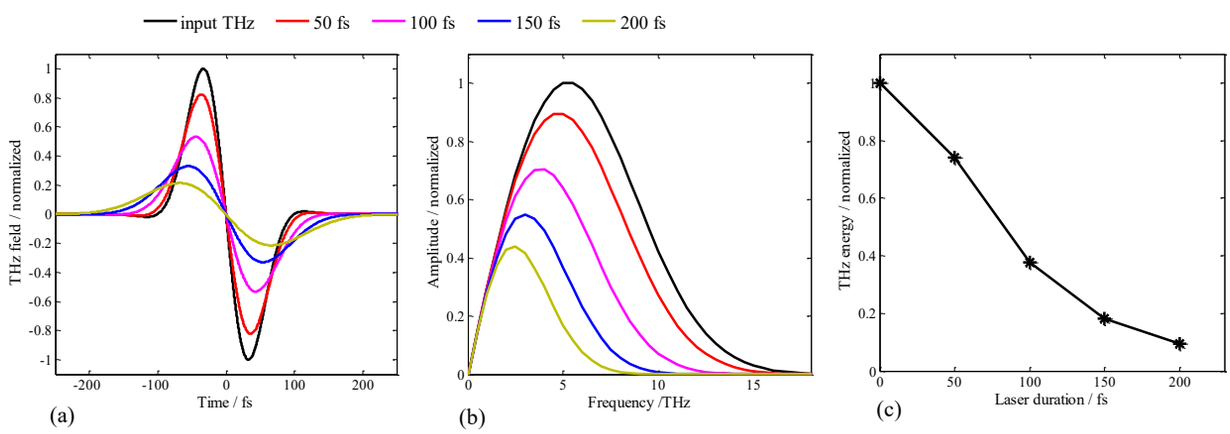

Fig. 3　The THz pulse distortions induced by air coherent detection technique with different probe laser pulses (50 fs, 100 fs, 150 fs, and 200 fs), the input THz pulse has a central frequency of 5 THz, (a) shows their time waveforms, (b) shows their frequency spectra, and (c) shows their pulse energy loss

图3　中心频率为5 THz的待探测的太赫兹脉冲在空气相干探测技术中使用不同脉宽(50 fs,100 fs,150 fs,200 fs)的探测激光引起的脉冲畸变,(a)为太赫兹脉冲波形,(b)为频谱分布,(c)为脉冲能量损失

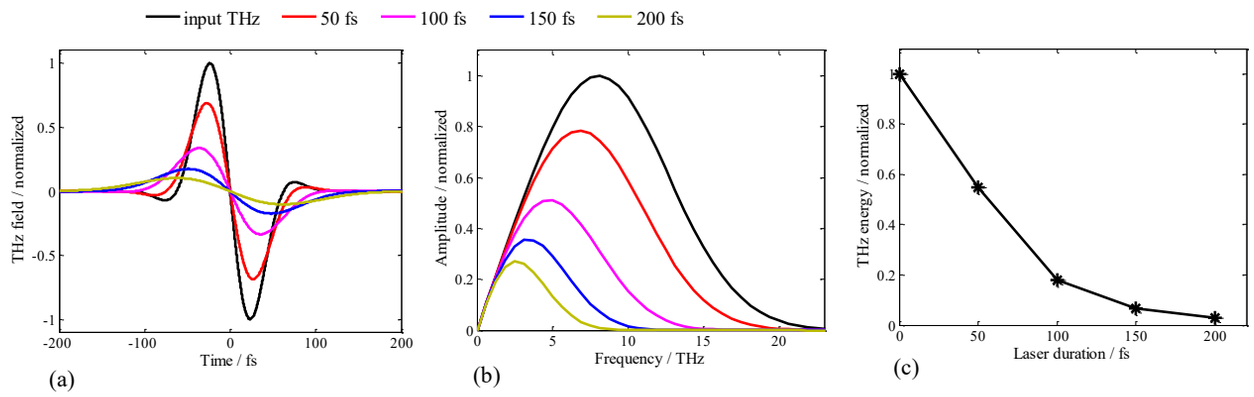

Fig. 4 The THz pulse distortion induced by the different probe laser pulses (50 fs, 100 fs, 150 fs, and 200 fs), the input THz pulse has a central frequency of 8 THz, (a) shows their time waveforms, (b) their frequency spectra, and (c) their pulse energy loss
图4 中心频率为8 THz的待探测太赫兹脉冲在空气相干探测技术中使用不同脉宽(50 fs,100 fs,150 fs,200 fs)的探测激光引起的脉冲畸变,(a)为太赫兹脉冲波形,(b)为频谱分布,(c)为脉冲能量损失

tection property as mentioned above, its performance in the frequency response is different from the Michelson interference system. The latter with a pyroelectrical detector or a bolometer also can measure the frequency spectrum of the far-infrared radiation with a much broadband response[23], but losing the phase information of the radiation. There are some reported different results between the air coherent detection technique and the Michelson interference. Andreev *et al*. have measured the THz radiation from the two-color laser induced plasma filament with these two methods, and the results clearly show that the high frequency range of THz waves from 5 THz to 10 THz is only obtained by the Michelson interference, as shown in Fig. 1(c) of their paper[24]. Since the THz redshift induced by the air coherent detection technique loses some high frequency components, as analyzed above. Koulouklidis *et al*. also have measured the THz radiation from the mid-infrared two-color plasma filament with the electro-optic sampling and the Michelson interference, the experimental result from the latter is much broader than the former[25].

The pyroelectric detector in the Michelson interference has broader and smoother frequency response, thus its measurement in the high frequency range is also sensitive. Meanwhile, the energy measurement of the broadband THz pulses with a pyroelectrical detector is more precise than that estimated by the air coherent detection technique. As pointed out by Fig. 2-5, there is somehow THz pulse energy loss produced by the air coherent detection process, and these simulated results can explain the experimental results reported before[26].

Although the air coherent detection technique does not have smooth response in the whole THz band, it is still a mature broadband coherent detection method. Its response is broader than the PCA and the EOS with a short femtosecond probe laser pulse (e. g. 50 fs). The generation and the detection of THz radiation based on the air plasma have offered a competitive way for the broadband THz spectroscopy system, and the experiment has shown its applications comparing with the conventional FTIR system[27]. The absorption coefficient and the refractive index of a sample in the THz range are usually obtained by comparing two THz signals, one is from the free space as the "reference", and the other is from the transmission (or reflective) as the "signal"[28]. Thus, both detected THz signals have experienced same interaction process of the detection system, meaning the same distortions. Thus, the ratio of the two THz signals in fact is not affected by these distortions. As a result, the measurement of the sample by the air coherent detection technique is still reliable. But the distortion and the energy loss should be considered when calibrating and measuring the new THz radiation source.

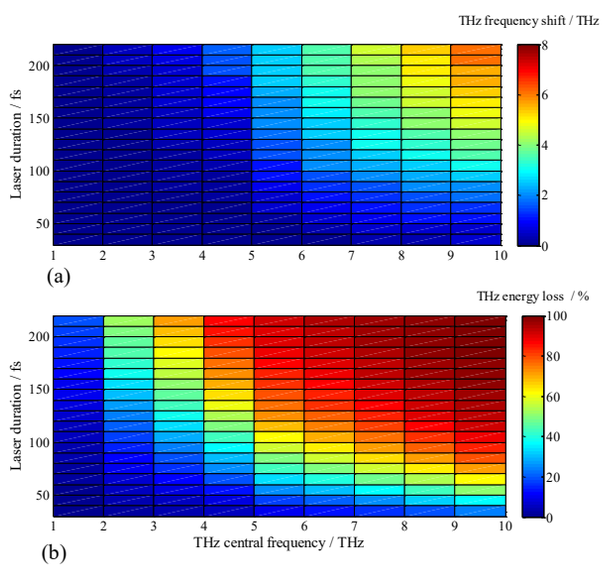

Fig. 5 The evolutions of THz pulse frequency redshift (a) and its pulse energy loss (b), X-axis is the central frequency of input THz pulses from 1 THz to 10 THz, and Y-axis is the duration of the probe laser pulses from 30 fs to 220 fs
图5 太赫兹脉冲频率红移(a)和脉冲能量损失(b)的演化趋势,X轴表示输入的太赫兹中心频率范围,1~10 THz,Y轴表示使用的探测激光脉冲范围,30~220 fs

4 Conclusions

In conclusion, the THz pulses distortions and the

energy loss induced by the air coherent detection technique during the detection process are studied and discussed based on the simulations. Three kinds of input broadband THz pulses with 2 THz, 5 THz, and 8 THz central frequency are given to show the details of the distortion and the pulse energy loss. Because the air coherent detection technique has high sensitivity in the low frequency range of THz waves, and low sensitivity in the high frequency range, it produces some redshift and pulse energy loss for the broadband THz pulses. This redshift and the energy loss vary with the duration of the probe laser pulse and the central frequency of THz pulse. Our calculations can explain the reported measurement difference between the Michelson interference and the air coherent detection technique. This work offers the quantitative clues to estimate the performance of the air coherent detection technique in the broad THz science and technology, especially to estimate the property of new broadband THz radiation sources.

References

[1] Mittleman D M. Perspective: terahertz science and technology [J]. *Journal of Applied Physics*, 2017, **122**(23): 230901.

[2] Dhillon S S, Vitiello M S, Linfield E H, *et al*. The 2017 terahertz science and technology roadmap [J]. *Journal of Physics D: Applied Physics*, 2017, **50**: 043001.

[3] Jepsen P U, Cooke D G, Koch M. Terahertz spectroscopy and imaging-modern techniques and applications [J]. *Laser & Photonics Review*, 2011, **5**(1): 124-166.

[4] Smith P R, Auston D H, Nuss M C. Subpicosecond photoconducting dipole antennas [J]. *IEEE Journal of Quantum of Electronics*, 1989, **24**(2): 255-260.

[5] Grischkowsky D, Ketchen M, Chi C C, *et al*. Capacitance free generation and detection of subpicosecond electrical pulses on coplanar transmission lines [J]. *IEEE Journal of Quantum of Electronics*, 1988, **24**(2): 221-225 (1988).

[6] Wu Q, Zhang X C. Free-space electro-optic sampling of terahertz beams [J]. *Applied Physics Letters*, 1995, **67**(24): 3523-3525.

[7] Nahata A, Auston D H, Heinz T F, *et al*. Coherent detection of freely propagation terahertz radiation by electro-optic sampling [J]. *Applied Physics Letters*, 1996, **68**(2): 150-152.

[8] Karpowicz N, Dai J M, Lu X, *et al*. Coherent heterodyne time-domain spectroscopy covering the entire "terahertz gap" [J]. *Applied Physics Letters*, 2008, **92**(1): 011131.

[9] Cook D J, Chen J X, Morlino E A, *et al*. Terahertz-field-induced second harmonic generation measurements of liquid dynamics, *Chemical Physics Letters*, 1999, 309: 221-228.

[10] Dai J M, Xie X, Zhang X C. Detection of broadband terahertz waves with a laser-induced plasma in gases [J]. *Physical Review Letters*, 2006, **97**(10): 103903.

[11] Dai J M, Clough B, Ho I, *et al*. Recent progresses in terahertz wave air photonics [J]. *IEEE Transactions on Terahertz Science and Technology*, 2011, **1**(1): 274-281.

[12] Du H W. Investigation on response function of terahertz air coherent detection technique [J]. *Applied Physics B*, 2020, **126**: 124.

[13] Gallot G, Grischkowsky D. Electro-optic detection of terahertz radiation [J]. *Journal of the Optical Society of America B-Optical Physics*, 1999, **16**(8): 1204-1212.

[14] Reimann K. Table-top sources of ultrashort THz pulses [J]. *Report on Progress in Physics*, 2007, **70**(10): 1597-1632.

[15] Sommer A, Bothschafter E M, Sato S A, *et al*. Attosecond nonlinear polarization and light-matter energy transfer in solids [J], *Nature*, 2016, **534**: 86-90.

[16] Hassan M T, Luu T T, Moulet A, *et al*. Optical attosecond pulses and tracking the nonlinear response of bound electrons [J]. *Nature*, 2016, **530**: 66-70.

[17] Gallot G, Zhang J, McGowan R W, *et al*. Measurements of the THz absorption and dispersion of ZnTe and their relevance to the electro-optic detection of THz radiation [J]. *Applied Physics Letters*, 1999, **74**(23): 3450-3452.

[18] Leitenstorfer A, Hunsche S, Shan J, *et al*. Detectors and sources for ultrabroadband electro-optic sampling: experiment and theory [J]. *Applied Physics Letters*, 1999, **74**(22): 1516-1518.

[19] Tilborg J, Schroeder C B, Filip C V, *et al*. Terahertz radiation as a bunch diagnostic for laser-wakefield-accelerated electron bunches [J]. *Physics of Plasma*, 2006, **13**(5): 056704.

[20] Casalbuoni S, Schlarb H, Schmidt B, *et al*. Numerical studies on the electro-optic detection of femtosecond electron bunches [J]. *Physical Review Special Topics-Accelerators and Beams*, 2008, **11**(7): 072802.

[21] Steffen B, Arsov V, Berden G, *et al*. Electro-optic time profile monitors for femtosecond electron bunches at the soft x-ray free electron laser FLASH [J]. *Physical Review Special Topics-Accelerators and Beams*, 2009, **12**(3): 032802.

[22] Walther M, Fischer B M, Ortner A, *et al*. Chemical sensing and imaging with pulsed terahertz radiation [J]. *Analytical and Bioanalytical Chemistry*, 2010, **397**: 1009-1017.

[23] Lewis R A. A review of terahertz detectors [J]. *Journal of Physics D: Applied Physics*, 2019, **52**: 433001.

[24] Andreeva V A, Kosareva O G, Panov N A, *et al*. Ultrabroad terahertz spectrum generation from an air-based filament plasma [J]. *Physical Review Letters*, 2016, **116**(6): 063902.

[25] Koulouklidis A D, Gollner C, Shumakova V, *et al*. Observation of extremely efficient terahertz generation from mid-infrared two-color laser filaments [J]. *Nature Communications*, 2020, **11**(1): 292-299.

[26] Du H W, Tang F, Zhang D Y, *et al*. Calibration of the field strength of broadband terahertz radiation in air coherent detection technique [J]. *Journal of Applied Physics*, 2018, **124**(14): 143101.

[27] Clough B, Dai J M, Zhang X C. Laser air photonics: beyond the terahertz gap [J]. *Materials Today*, 2012, **15**(1): 50-58.

[28] Jepsen P U. Phase retrieval in terahertz time-domain measurements: a "how to" tutorial [J]. *Journal of Infrared, Millimeter, and Terahertz Waves*, 2019, **40**(4): 395-411.